THE PLASMA FOCUS- TRENDING INTO THE FUTURE

S Lee[1,2,3] and S H Saw[1,2]

[1]INTI University College, 71800 Nilai, Malaysia

[2] Institute for Plasma Focus Studies, 32 Oakpark Drive, Chadstone, VIC3148, Australia

[3] Nanyang Technological University, National Institute of Education, Singapore 637616

Abstract

The plasma focus is a promising small scale alternative to the huge Tokamak project in the development of nuclear fusion energy. Its strength lies in the characteristic that the plasma condition is the same whether the plasma focus is a small sub-kilojoule machine or a large one with thousands of kilojoules of stored energy; and the related constancy of the dynamic resistance. Yet this strength turns out to result in a weakness. The observed neutron 'saturation' is more correctly stated as a 'scaling deterioration' effect. This critical weakness is due to the same constancy of plasma condition intimately related to a constancy of the dynamic resistance. The understanding of this situation points to a new class of plasma focus devices to overcome the 'saturation' of the electric current. Plasma focus technology has to move to ultra high voltage technology and take advantage of circuit manipulation techniques in order to move into a new era of high performance. This paper will examine fundamental scaling properties of the plasma focus including speeds, temperatures, dimensions and times. It will link up these basic scaling characteristics with the crucial ideas of the inherent yield scaling deterioration, thus providing a clear understanding of its overall performance characteristics, paving the way for future exploitation.

Keywords: Plasma Focus, Nuclear Fusion, Plasma Focus Scaling, Plasma Focus Properties, Neutron Saturation

1. Introduction

The plasma focus is one of the smaller scale devices which complement the international efforts to build a nuclear fusion reactor [1]. It is an important device for the generation of intense multi-radiation including x-rays, particle beams and fusion neutrons. The physics underlying the mechanisms for the generation of these radiations in the plasma focus is still not completely known although there have been intensive investigations for the past five decades. Experimental and theoretical work on the focus has reached quite high levels. For example, detailed simulation, work on the plasma focus had been carried out since 1971 [2] and a large range of devices has been constructed from less than 100 J small focus to greater than 1 MJ large focus [3]. Advanced experiments have been carried out on the dynamics, radiation, instabilities and non-linear phenomena [4]. Yet despite all these intensive studies, very little regarding scaling appears to be documented with the exception of the scaling law for neutron yield. Other more recent work has thrown much needed light on other aspects of scaling such as how the dimensions of the dense focused plasma (the focus pinch) and the pinch lifetime scale with apparatus dimensions, the dominating dimension being the anode radius [5].

2. Neutron Scaling with Energy

Historically the most appealing quantity for use as the base for scaling is the stored energy used to drive the focus. Using the highest voltage technologically convenient all one needs to do to scale up energy ($E_0=0.5C_0V_0^2$) is to put in more capacitors in parallel, thus increasing the capacitance of the energy bank and incidentally also decreasing the static inductance L_0 of the bank to some extent. Thus this has become a major preoccupation of the larger laboratories, sometimes seemingly at the expense of other considerations. Along these lines, early work has shown that $Y_n \sim E_0^2$; and since under ideal conditions (minimized inductance L_0 and when the system is dominated by the generator impedance) the capacitor current I may have the relationship $I \sim E^{0.5}$, then it quickly follows that $Y_n \sim I^4$. This very simplistic view has been too smug and has led to the hold-up of the progress of large plasma focus devices. It was found that when the capacitor bank reached storage energies of only several hundred kJ, the neutron yield no longer increased, the so-called neutron saturation effect. It has been shown recently that whilst the discharge circuit is indeed dominated by the generator impedance at low energies, i.e. low capacitance so that indeed $I \sim E^{0.5,}$ at a certain point when the C_0 i.e. E_0

gets sufficiently big, the generator impedance has dropped to such low values as to reach the value of the load impedance that the generator is driving. As E_0 is increased even further and further, the generator impedance eventually becomes negligible when compared to the load impedance which remains relatively constant, hardly affected by the decreasing generator impedance. Eventually at very large E_0, the constant load impedance completely dominates and the circuit current reaches an asymptotic value and does not even increase at all for a further increase in E_0 at those already very large values. At this point typically in the high tens of MJ for the plasma focus, the capacitor current may be considered to have saturated, leading to neutron saturation. What is observed at hundreds of kJ and which has been termed as neutron saturation is based on very limited data. When more data from more experiments are put in together with data from rigorous systematic numerical experiments, then the global picture shows the scaling deterioration very clearly (see Figure 1). We will come back to this central problem again in the concluding section of this paper.

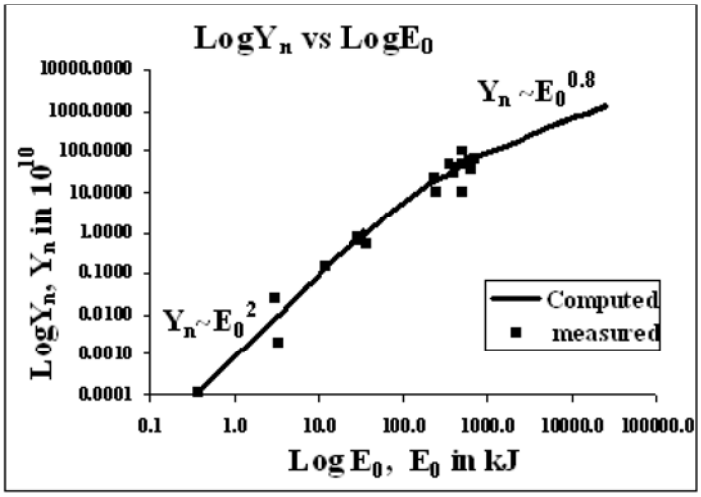

Figure 1. The global scaling law, combining experimental and numerical data. The global data illustrates Y_n scaling observed in numerical experiments from 0.4 kJ to 25 MJ (solid line) using the Lee model code, compared to measurements compiled from publications (squares) of various machines from 0.4 kJ to 1 MJ.

3. Scaling Properties of the Plasma Focus

3.1. Various plasma focus devices

In Figure 2a is shown the UNU ICTP PFF 3 kJ device [6] mounted on a 1m by 1m by 0.5m trolley, which was wheeled around the ICTP for the 1991 and 1993 Plasma Physics Colleges. The single capacitor is seen in the picture mounted on the trolley. In contrast, Figure 2b shows the 300-times larger PF1000, the 1 MJ device at the ICDMP in Warsaw Poland [7]. Only the chamber and the cables connecting the plasma focus to the capacitors are shown. The capacitor bank with its 288 capacitors, switches and chargers are located in a separate hall.

Figure 2a. 3 kJ UNU ICTP PFF

Figure 2b. 1 MJ PF1000 plasma focus

We show in Table 1 the characteristics of three plasma focus devices [8] computed using the Lee model code, fitted by comparing the computed current waveform to the measured current waveform. These computed characteristics are also in broad agreement with measured experimental values where available in the published literature [6,7,9].

Table 1.

	E_0	a	z_0	V_0	P_0	I_{peak}	v_a	ID	SF	Y_n
	kJ	cm	cm	kV	Torr	kA	cm/□s	kA/cm	(kA/cm) $torr^{0.5}$	10^8
PF1000	486	11.6	60	27	4	1850	11	160	85	1100
UNU ICTP	2.7	1.0	15.5	14	3	164	9	173	100	0.20
PF-400J	0.4	0.6	1.7	28	7	126	9	210	82	0.01

In Table 1 we look at the PF1000 and study its properties at typical operation with device storage at 500 kJ level. We compare this big focus with two small devices at the kJ level.

From Table 1 we note:

Voltage and pressure do not have any particular relationship to E_0.
Peak current I_{peak} increases with E_0.
Anode radius 'a' increases with E_0.
Current per cm of anode radius (ID) I_{peak}/a is in a narrow range 160 to 210 kA/cm
SF (speed or drive factor) $(I_{peak}/a)/P_0^{0.5}$ is 82 to 100 (kA/cm) $torr^{0.5}$ deuterium gas. Observed Peak axial speed v_a is in the narrow range 9 to 11 cm/us.

Fusion neutron yield Y_n ranges from 10^6 for the smallest device to 10^{11} for the PF1000.

We stress that whereas the ID and SF are practically constant at around 180 kA/cm and 90 (kA/cm) per $torr^{0.5}$ deuterium gas throughout the range of small to big devices, Y_n changes over 5 orders of magnitude.

We emphasise that the data of Table 1 is generated from numerical experiments and most of the data has been confirmed by actual experimental measurements and observation.

Table 2.

	c= b/a	a	T_{pinch}	v_p	r_{min}	z_{max}	Pinch duration	r_{min}/a	z_{max}/a	Pinch duration/a
		cm	10^6K	cm/□s	cm	cm	ns			ns/cm
PF1000	1.4	11.6	2	13	2.2	19	165	0.17	1.6	14
UNU ICTP PFF	3.4	1.0	8	26	0.13	1.4	7.3	0.14	1.4	8
PF400J	2.6	0.6	6	23	0.09	0.8	5.2	0.14	1.4	9

Table 2 compares further the properties of the range of plasma focus devices. The properties being compared in this table are mainly related to the radial phase. These are computed from numerical experiments and found to be in close agreement with laboratory measurements [5,10].

The pinch temperature T_{pinch} is strongly correlated to the square of the radial pinch speed v_p.
v_p itself is closely correlated to the value of v_a and c=b/a; so that for a constant v_a, v_p is almost proportional to the value of c [11].

Notably the dimensions and lifetime of the focus pinch scales as the anode radius 'a'.
r_{min}/a (almost constant at 0.14-0.17)
z_{max}/a (almost constant at 1.5)
Pinch duration has a relatively narrow range of 8-14 ns/cm of anode radius.
The duration per unit anode radius is correlated to the inverse of T_{pinch}.

T_{pinch} itself is a measure of the energy per unit mass. It is quite remarkable that this energy density at the focus pinch varies so little (factor of 5) over a range of device energy of more than 3 orders of magnitude (factor of 1000).

This practically constant pinch energy density (per unit mass) is related to the constancy of the axial speed moderated by the effect of the values of c=b/a on the radial speed.

The constancy of r_{min}/a suggests that the devices also produce the same compression of ambient density to maximum pinch density; with the ratio (maximum pinch density)/(ambient density) being proportional to $(a/r_{min})^2$. So for two devices of different sizes starting with the same ambient fill density, the maximum pinch density would be the same.

From the above discussion, we may put down as rule-of-thumb the following scaling relationships, subject to minor variations caused primarily by the variation in c.

Axial phase energy density (per unit mass)	constant
Radial phase energy density (per unit mass)	constant
Pinch radius ratio	constant
Pinch length ratio	constant
Pinch duration per unit anode radius	constant

Summarising, the dense hot plasma pinch of a small E_0 plasma focus and that of a big E_0 plasma focus have essentially the same energy density, the same mass density. The big E_0 plasma focus has a bigger physical size and a bigger discharge current. The size of the plasma pinch scales proportionately to the current and to the anode radius, as does the duration of the plasma pinch. The bigger E_0, the bigger I_{peak}, the bigger 'a' has to be, hence the larger the plasma pinch and the longer the duration of the plasma pinch. The larger size and longer duration of the big E_0 plasma pinch are essentially the properties leading to the bigger neutron yield compared to the yield of the small E_0 plasma focus.

We may also summarise the dimensions and lifetimes for deuterium and neon plasma focus pinch as follows [5,10]:

Table 3.

		Deuterium	**Neon (for SXR)**
minimum radius	r_{min}	0.15a	0.05a
max length (hollow anode)	z	1.5a	1.6a
radial shock transit	t_{comp}	$5x10^{-6}a$	$4x10^{-6}a$
pinch lifetime	t_p	$10^{-6}a$	$10^{-6}a$
Speed factor	SF	90	

where, for the times in sec, the value of anode radius, a, is in m. For the neon calculations radiative terms are included; and the stronger compression (smaller radius) is due to thermodynamic effects. The units of the speed factor SF are: $(kA/cm)/(torr^{0.5})$

The above description of the plasma focus combines data from numerical experiments, consistent with laboratory observations [5,8,10,11].

The next section describes briefly the code.

4. Introduction to the Lee model code

The Lee model code couples the electrical circuit with plasma focus dynamics, thermodynamics, and radiation, enabling a realistic simulation of all gross focus properties. The basic model, described in 1984 [12], was successfully used to assist several projects [6,13,14]. Radiation-coupled dynamics was included in the five-phase code, leading to numerical experiments on radiation cooling [15]. The vital role of a finite small disturbance speed discussed by Potter in a *Z*-pinch situation [16] was incorporated together with real gas thermodynamics and radiation-yield terms. This version of the code assisted other research projects [17-22] and was web published in 2000 [23] and 2005 [24]. Plasma self-absorption was included in 2007 [23], improving the SXR yield simulation. The code has been used extensively in several machines including UNU/ICTP PFF [6,15,17,19,20-22,25], NX2 [18,26,27], and NX1 [27,28] and has been adapted for the Filippov-type plasma focus DENA [29]. A recent development is the inclusion of the neutron yield Y_n using a beam–target mechanism [30-34], incorporated in recent versions [8,11] of the code (versions later than RADPFV5.13), resulting in realistic Y_n scaling with I_{pinch} [30,31]. The versatility and utility of the model are demonstrated in its clear distinction of I_{pinch} from I_{peak} [32] and the recent uncovering of a plasma focus pinch current limitation effect [33-36], as static inductance is reduced towards zero. Extensive numerical experiments had been carried out systematically resulting in the uncovering of neutron [1,30,31, 37-39] and SXR [40-43] scaling laws over a wider range of energies and currents than attempted before. The numerical experiments also gave insight into the nature and cause of 'neutron saturation [31,38,44]. The description, theory, code, and a broad range of results of this "Universal Plasma Focus Laboratory Facility" are available for download from [8,11].

A brief description of the 5-phase model is given in the following.

4.1 The 5-phases

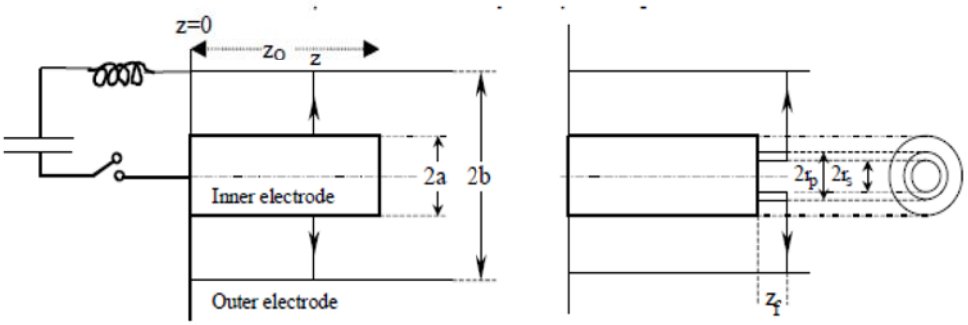

Figure 3. Schematic of the axial and radial phases. The left section depicts the axial phase, the right section the radial phase. In the left section, z is the effective position of the current sheath-shock front structure. In the right section r_s is the position of the inward moving shock front driven by the piston at position r_p. Between r_s and r_p is the radially imploding slug, elongating with a length z_f. The capacitor, static inductance and switch powering the plasma focus is shown for the axial phase schematic only.

The five phases (*a-e*) are summarised [11,35,38,45,46] as follows:
a. Axial Phase (see Figure 3 left part): Described by a snowplow model with an equation of motion which is coupled to a circuit equation. The equation of motion incorporates the axial phase model parameters: mass and current factors f_m and f_c. The mass swept-up factor f_m accounts for not only the porosity of the current sheet but also for the inclination of the moving current sheetshock front structure, boundary layer effects, and all other unspecified effects which have effects equivalent to increasing or reducing the amount of mass in the moving structure, during the axial phase. The current factor f_c accounts for the fraction of current effectively flowing in the moving structure (due to all effects such as current shedding at or near the back-wall, and current sheet inclination). This defines the fraction of current effectively driving the structure, during the axial phase.

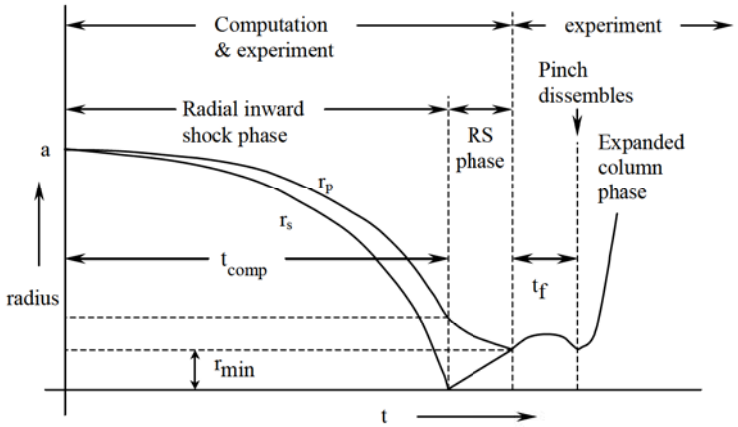

Figure 4. Schematic of radius versus time trajectories to illustrate the radial inward shock phase when r_s moves radially inwards, the reflected shock (RS) phase when the reflected shock moves radially outwards, until it hits the incoming piston r_p leading to the start of the pinch phase (t_f) and finally the expanded column phase.

b. Radial Inward Shock Phase (see Figure 3 right part, also Figure 4): Described by 4 coupled equations using an elongating slug model. The first equation computes the radial inward shock speed from the driving magnetic pressure. The second equation computes the axial elongation speed of the column. The third equation computes the speed of the current sheath, (magnetic piston), allowing the current sheath to separate from the shock front by applying an adiabatic approximation [16]. The fourth is the circuit equation. Thermodynamic effects due to ionization and excitation are incorporated into these equations, these effects being particularly important for gases other than hydrogen and deuterium. Temperature and number densities are computed during this phase using shock-jump equations. A communication delay between shock front and current sheath due to the finite small disturbance speed [11,16, 46] is crucially implemented in this phase. The model parameters, radial phase mass swept-up and current factors f_{mr} and f_{cr} are incorporated in all three radial phases. The mass swept-up factor f_{mr} accounts for all mechanisms which have effects equivalent to increasing or reducing the amount of mass in the moving slug, during the radial phase. The current factor f_{cr} accounts for the fraction of current effectively flowing in the moving piston forming the back of the slug (due to all effects). This defines the fraction of current effectively driving the radial slug.

c. Radial Reflected Shock (RS) Phase (See Figure 4): When the shock front hits the axis, because the focus plasma is collisional, a reflected shock develops which moves radially outwards, whilst the radial current sheath piston continues to move inwards. Four coupled equations are also used to describe this phase, these being for the reflected shock moving radially outwards, the piston moving radially inwards, the elongation of the annular column and the circuit. The same model parameters f_{mr} and f_{cr} are used as in the previous radial phase. The plasma temperature behind the reflected shock undergoes a jump by a factor close to 2. Number densities are also computed using the reflected shock jump equations.

d. Slow Compression (Quiescent) or Pinch Phase (See Figure 4): When the out-going reflected shock hits the inward moving piston, the compression enters a radiative phase in which for gases such as neon, radiation emission may actually enhance the compression where we have included energy loss/gain terms from Joule heating and radiation losses into the piston equation of motion. Three coupled equations describe this phase; these being the piston radial motion equation, the pinch column elongation equation and the circuit equation, incorporating the same model parameters as in the previous two phases. The duration of this slow compression phase is set as the time of transit of small disturbances across the pinched plasma column. The computation of this phase is terminated at the end of this duration.

e. Expanded Column Phase: To simulate the current trace beyond this point we allow the column to suddenly attain the radius of the anode, and use the expanded column inductance for further integration. In this final phase the snow plow model is used, and two coupled equations are used similar to the axial phase above. This phase is not considered important as it occurs after the focus pinch.

We note [45] that in radial phases *b, c* and *d*, axial acceleration and ejection of mass caused by necking curvatures of the pinching current sheath result in time-dependent strongly center-peaked density distributions. Moreover the transition from phase *d* to phase *e* is observed in laboratory measurements to occur in an extremely short time with plasma/current disruptions resulting in localized regions of high densities and temperatures. These centre-peaking density effects and localized regions are not modeled in the code, which consequently computes only an average uniform density and an average uniform temperature which are considerably lower than measured peak density and temperature. However, because the four model parameters are obtained by fitting the computed total current waveform to the measured total current waveform, the model incorporates the energy and mass balances equivalent, at least in the gross sense, to all the processes which are not even specifically modeled. Hence the computed gross features such as speeds and trajectories and integrated soft x-ray yields have been extensively tested in numerical experiments for several machines and are found to be comparable with measured values.

4.2 The model code as a general diagnostic tool

The model code now includes a sheet in which is displayed charts of the properties of the particular shot including: total discharge current and plasma current, tube voltage, axial trajectories and speeds, tube inductance and total inductive energy, piston work and Joule work related to the dynamic resistance, the dynamic resistance, ion and electron number density (spatial uniform averaged and peak) , plasma temperature (spatial uniform averaged and peak), computed soft x-ray power; all these properties are displayed as functions of time, in the axial phase (where applicable) and in the radial phase. The model code thus provides information to guide experimental measurements and in this sense can be considered as a powerful diagnostics tool as well [38].

5. Neutron Saturation- Its Relationship with the Plasma Focus Properties

In Section 2 we had discussed the global scaling law for neutron yield as shown in Figure 1 which was compiled with data from experiments and numerical experiments. Figure 1 shows that whereas at energies up to tens of kJ the $Y_n \sim E_0^2$ scaling held, deterioration of this scaling became apparent above the low hundreds of kJ. This deteriorating trend worsened and tended towards $Y_n \sim E_0^{0.8}$ at tens of MJ. The global data of Figure 1 suggests that the apparently observed neutron saturation effect is overall not in significant variance with the deterioration of the scaling shown by the numerical experiments.

5.1. The cause of neutron 'saturation' is the dynamic resistance

A simple yet compelling analysis of the cause of this neutron saturation has been published [44]. In that paper it is shown that it is the interaction of dynamic resistance of the plasma focus axial phase with the generator impedance of the plasma focus capacitor bank that causes the deterioration of the scaling trend and eventual saturation of yield at high multi-MJ energies. This dynamic resistance is practically a constant over the range of plasma focus devices, depending as it is on the value of ln(c) (where radius ratio c=b/a) and on the axial speed; the latter being practically a constant and the c having only a small range typically from 1.5 to 3. The value of this dynamic resistance is typically 5

m□. The value of the generator impedance of the capacitor bank on the other hand is $Z_0=(L_0/C_0)^{0.5}$, inversely proportional to $C_0^{0.5}$ and is much larger than the dynamic resistance for small plasma focus whilst being much smaller than the dynamic resistance for large plasma focus devices as C_0 is increased from the range of □F to the range of tens of thousands of □F. It turns out that in the region of kJ to tens of kJ the scaling of the current is controlled by the bank impedance. In this range of energy the current thus increases with $C_0^{0.5}$. On the other hand at very large MJ energies the capacitor bank impedance has dropped so much below the dynamic resistance that the circuit current is now controlled solely by the dynamic resistance. As this is a constant, increasing the capacitance or bank energy any further no longer affects the circuit current which then tends to an asymptotic value. The point at which the current scaling begins to deteriorate is in the range of low hundreds of kJ. As bank energy increases to this range of energies, the scaling of current begins to deteriorate; the deterioration worsens as MJ levels are approached; but it is not until the high tens of MJ that circuit current begins to approach saturation. Likewise the behavious of the neutron yield. Thus the term neutron 'saturation' popularly referred to in the literature at several hundred kJ is a misnomer, mistakenly applied to what is in fact just a neutron yield scaling deterioration.

The asymptotic value at high tens of MJ is $I_{peak}=V_0/Z_{total} \sim V_0/DR_0$ where V_0 is charging voltage, Z_{total} is total circuit impedance which tends towards the value of the axial phase dynamic resistance DR_0 since at very large values of C_0 the value of $Z_0=(L_0/C_0)^{0.5} << DR_0$. Thus DR_0 causes current 'saturation'. This is shown in Figure 5.

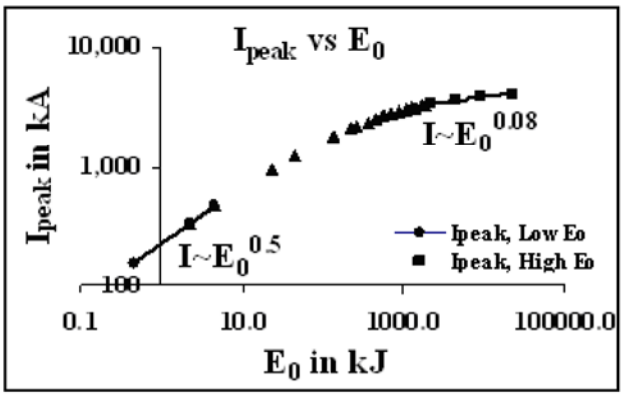

Figure 5. I_{peak} versus E_0 on log-log scale, illustrating I_{peak} 'saturation' at large E_0

In other extensive numerical experiments we had shown the following relationships between Y_n and I_{peak} and I_{pinch} as follows:

$$Y_n \sim I_{pinch}^{4.5} \quad (1)$$

$$Y_n \sim I_{peak}^{3.8} \quad (2)$$

Hence saturation of I_{peak} will lead to saturation of Y_n.
Thus we have shown that neutron 'saturation' is inevitable as E_0 is increased to very large values by an increase in C_0; simply due to the dominance of the axial phase dynamic resistance. However the apparently observed neutron 'saturation' at low hundreds of kJ is more accurately represented as a neutron scaling deterioration.

5.2. Relationship with plasma focus scaling properties

Now we link up this neutron scaling law deterioration and subsequent saturation with the scaling properties of the plasma focus discussed in Section 3. This scaling law deterioration and saturation is due to the constancy of the speed factor SF and energy density, as E_0 increases. The constancy of the axial speed or SF caused the deterioration of current scaling, requiring that the anode radius 'a' is not increased as much as it would have been increased if there were no deterioration. This implies that the size and duration of the focus pinch are also restricted by the scaling deterioration. Ultimately at high tens of MJ, I_{peak} saturates, the anode radius of the focus should not be increased anymore with E_0. The size and duration of the focus pinch no longer increase with E_0 and Y_n also saturates. We now have the complete picture.

6. Conclusions

This paper has reviewed the global scaling law for neutron yield as a function of storage energy. First, the scaling deterioration and eventual 'saturation' of circuit current are ascribed to the energy density constancy manifested in the form of a constancy in dynamic resistance of the axial phase. Second, the deterioration of current scaling implies that the anode radius 'a' is not increased as much as it would have been if there were no deterioration. Third, this implies

that the size and duration of the focus pinch are also restricted by the scaling deterioration. Ultimately at high tens of MJ, I_{peak} saturates, the anode radius of the focus should not be increased anymore with E_0, the size and duration of the focus pinch no longer increase with E_0.

The restriction on the plasma pinch size and duration has a corresponding effect on the neutron yield Y_n. The neutron yield Y_n scales with E_0^2 at low energies up to tens of kJ, begins to exhibit scaling deterioration around low hundreds of kJ and approaches 'saturation' at high tens of MJ.

In this manner this paper has for the first time connected the global scaling laws for the current and the neutron yield to the scaling properties of the plasma focus. This more complete picture will facilitate the further development of the plasma focus as a fusion device.

References

[1] Lee S. Nuclear fusion and the Plasma Focus. Invited paper Tubav Conferences: Nuclear & Renewable Energy Sources Ankara, Turkey, 28 & 29 September 2009. Procs:pg 9-18

[2] D E Potter Numerical Studies of the Plasma Focus Phys. Fluids 14, 1911-1914 (1971)

[3] Leopoldo Soto. New trends and future perspectives on plasma focus research 2005 *Plasma Phys. Control. Fusion* 47 A361

[4] Bernard A., Bruzzone H., Choi P., Chuaqui H., Gribkov V., Herrera J., Hirano K., Krejci A., Lee S., Luo C.et al Scientific Status of Plasma focus Research. *Moscow J Physical Society,* 1998, 8, 93-170.

[5] Lee S. and Serban A., "Dimensions and lifetime of the plasma focus pinch," *IEEE Trans. Plasma Sci.*, 1996, *24*, no. 3, pp. 1101–1105, Jun. 1996.

[6] Lee, S.; Tou, T. Y.; Moo, S. P.; Eissa, M. A.; Gholap, A. V.; Kwek, K. H.; Mulyodrono, S.; Smith, A. J.; Suryadi,
S.; Usada, W.;. Zakaullah, M. A simple facility for the teaching of plasma dynamics and plasma nuclear fusion. *Amer. J. Phys.* 1988, *56,* no. 1, 62–68.

[7] Gribkov V. A., Banaszak A., Bienkowska B., Dubrovsky A. V, Ivanova-Stanik I., Jakubowski L., Karpinski L., Miklaszewski R. A., Paduch M., Sadowski M. J., Scholz M., Szydlowski A., and Tomaszewski K., "Plasma dynamics in the PF-1000 device under fullscale energy storage: II. Fast electron and ion characteristics versus neutron emission parameters and gun optimization perspectives," *J. Phys. D,Appl. Phys.*, 2007, *40*, no. 12, pp. 3592–3607.

[8] Web-site: http://www.intimal.edu.my/school/fas/UFLF/

[9] Silva P, Moreno J, Soto L, Birstein L, Mayer R E and Kies W 2003. *Appl. Phys. Lett*. 83 3269

[10] Lee, S *Characterising the Plasma Focus Pinch and Speed Enhancing the Neutron Yield.* In: First Cairo Conference on Plasma Physics & Applications. 11-15 October 2004. International Cooperation Bilateral Seminars (Vol 34). Forschungszentrum Juelich GmbH, Juelich, Germany, pp. 27-33. ISBN 3-89336-374-2

[11] Lee S. Radiative Dense Plasma Focus Computation Package: RADPF, 2009
http://www.plasmafocus.net
http://www.plasmafocus.net/IPFS/modelpackage/File1RADPF.htm
http://www.plasmafocus.net/IPFS/modelpackage/File2Theory.pdf
http://www.plasmafocus.net/IPFS/modelpackage/UPF.htm

[12] Lee, S. Plasma focus model yielding trajectory and structure. In *Radiations in Plasmas*, McNamara, B., Ed.; World Scientific, Singapore: 1984; Volume II, pp. 978–987.

[13] Tou, T. Y.; Lee, S.; Kwek, K. H. Non perturbing plasma focus measurements in the run-down phase. *IEEE Trans. Plasma Sci.* 1989, *17*, no. 2, 311–315.

[14] Lee, S. A sequential plasma focus. *IEEE Trans. Plasma Sci.* 1991, *19*, no.5, 912–919.

[15] Jalil bin Ali. *Development and studies of a small plasma focus*, Ph.D. Dissertation; Universiti Teknologi Malaysia, Malaysia, 1990.

[16] Potter, D. E. The formation of high-density z-pinches. *Nucl. Fusion.* 1978, *18*, 813–823.

[17] Liu M., "Soft X-rays from compact plasma focus," Ph.D. dissertation, NIE, Nanyang Technological Univ., Singapore, 2006. ICTP Open Access Archive. [Online]. Available: http://eprints.ictp.it/327/

[18] Bing S., "Plasma dynamics and X-ray emission of the plasma focus," Ph.D. dissertation, NIE, Nanyang Technological Univ., Singapore, 2000. ICTP Open Access Archive. [Online]. Available: http://eprints.ictp.it/99/

[19] Serban A. and Lee S., "Experiments on speed-enhanced neutron yield from a small plasma focus," *J. Plasma Phys.*, 1998, *60*, no. 1, pt. 1, pp. 3–15, Aug. 1998.

[20] Liu M.H., Feng X.P., S. V. Springham, and Lee S., "Soft X-ray measurement in a small plasma focus operated in neon," *IEEE Trans. Plasma Sci.*, 1998, *26*, no. 2, pp. 135–140.

[21] Lee S., in *Twelve Years of UNU/ICTP PFF—A Review*. Trieste, Italy: Abdus Salam ICTP, 1998, pp. 5–34. IC/98/
231, ICTP Open Access Archive. [Online]. Available: http://eprints.ictp.it/31/

[22] Springham S. V., Lee S., and Rafique M. S., "Correlated deuteron energy spectra and neutron yield for a 3 Kj plasma focus," *Plasma Phys. Control. Fusion*, 2000, 42, no. 10, pp. 1023–1032.

[23] Lee S., 2000–2007. [Online]. Available: http://ckplee.myplace.nie.edu.sg/plasmaphysics/

[24] Lee S., *ICTP Open Access Archive*, 2005. [Online]. Available: http://eprints.ictp.it/85/

[25] Mohammadi M. A., Sobhanian S., Wong C. S., Lee S., Lee P., and Rawat R. S., "The effect of anode shape on neon soft X-ray emissions and current sheath configuration in plasma focus device," *J. Phys. D, Appl. Phys.*, 2009, *42*, no. 4, 045 203 (10pp).
[26] Wong D., Lee P., Zhang T., Patran A., Tan T. L., Rawat R. S., and Lee S., "An improved radiative plasma focus model calibrated for neonfilled NX2 using a tapered anode," *Plasma Sources Sci. Technol.*, 2007. *16*, no. 1, pp. 116 123.
[27] Lee S., P. Lee, Zhang G., Feng X., Gribkov V. A., Liu M., Serban A., and Wong T., "High rep rate high performance plasma focus as a powerful radiation source," *IEEE Trans. Plasma Sci.*, 1998, *26*, no. 4, pp. 1119–1126.
[28] Bogolyubov E. P., Bochkov V. D., Veretennikov V. A., Vekhoreva L. T., Gribkov V. A., Dubrovskii A. V., Ivanov Y. P., Isakov A. I, Krokhin O. N., Lee P., Lee S., Nikulin V. Y., Serban A., Silin P. V., Feng X., and Zhang G. ,X., "A powerful soft X-ray source for X-ray lithography based on plasma focusing," *Phys. Scr.*, 1998, *57*, no. 4, pp. 488–494.
[29] Siahpoush V., Tafreshi M. A., Sobhanian S., and Khorram S., "Adaptation of Sing Lee's model to the Filippov type plasma focus geometry," *Plasma Phys. Control. Fusion*, 2005, *47*, no. 7, pp. 1065–1075.
[30] Lee S. and Saw S. H., "Neutron scaling laws from numerical experiments," *J. Fusion Energy*, 2008, *27*, no. 4, pp. 292–295.
[31] Lee S., "Current and neutron scaling for megajoule plasma focus machines," *Plasma Phys. Control. Fusion*, 2008,
50, no. 10, p. 105 005 (14pp).
[32] Lee S., Saw S. H., Lee P. C. K., Rawat R.S., and Schmidt H., "Computing plasma focus pinch current from total current measurement," *Appl. Phys. Lett.*, 2008, *92*, no. 11, p. 111 501.
[33] Lee S. and Saw S. H., "Pinch current limitation effect in plasma focus," *Appl. Phys. Lett.*, 2008, *92*, no. 2, p. 021 503.
[34] Lee S., Lee P., Saw S. H., and Rawat R. S., "Numerical experiments on plasma focus pinch current limitation," *Plasma Phys. Control. Fusion*, 2008, *50*, no. 6, 065 012 (8pp).
[35] Internet Workshop on Plasma Focus Numerical Experiments (IPFS-IBC1) 14 April-19 May 2008

http://www.plasmafocus.net/IPFS/Papers/IWPCAkeynote2ResultsofInternet- basedWorkshop.doc
[36] Akel M., Al-HIawat Sh., Lee S. "Pinch Current and Soft x-ray yield limitation by numerical experiments on Nitrogen Plasma Focus". *J Fusion Energy* DOI 10.1007/s10894-009-9238-6. First online 21 August 2009
[37] Saw S. H. and Lee S. "Scaling laws for plasma focus machines from numerical experiments". Invited paper: IWPDA, Singapore 2&3 July 2009
[38] Lee S. Diagnostics and Insights from Current waveform and Modelling of Plasma Focus. Keynote address: IWPDA, Singapore 2-July 2009
[39] Saw S. H. and Lee S. "Scaling the plasma focus for fusion energy considerations". Tubav Conferences: Nuclear &
Renewable Energy Sources, Ankara, Turkey, 28 & 29 September 2009.
[40] Lee S., Saw S. H., Lee P. & Rawat R. S., "Numerical Experiments on Neon plasma focus soft x-rays scaling", *Plasma Physics and Controlled Fusion*, 2009, *51*, 105013 (8pp).
[41] Akel M., Al-Hawat Sh., Lee S. "Numerical Experiments on Soft X-ray Emission Optimization of Nitrogen Plasma
in 3 kJ Plasma Focus SY-1 Using Modified Lee Model", *J Fusion Energy* DOI 10.1007/s10894-009-9203-4 First online, May 19, 2009.
[42] M. Akel, Sh. Al-Hawat, S. H. Saw and S. Lee. Numerical Experiments on Oxygen Soft X-Ray Emissions from Low Energy Plasma Focus Using Lee Model. Journal of Fusion Energy DOI 10.1007/s10894-009-9262-6 First online 22 November 2009
[43] Lee S., Rawat R. S., Lee P., S H Saw S. H., Soft x-ray yield from NX2 plasma focus, *JOURNAL OF APPLIED PHYSICS*, 2009, *106*, 023309.
[44] Lee S. "Neutron Yield Saturation in Plasma Focus-A fundamental cause" *APPLIED PHYSICS LETTERS*, 2009, *95*, 151503 published online 15 October 2009
[45] Saw S. H., Lee P. C. K., Rawat R. S. & Lee S. 2009 'Optimizing UNU/ICTP PFF Plasma Focus for Neon Soft X ray Operation' *IEEE Trans on Plasma Sc*, 2009, *37*, 1276-1282.
[46] Lee S., Saw S. H., Soto L., Moo S. P., Springham S. V., Numerical experiments on plasma focus neutron yield versus pressure compared with laboratory experiments, *Plasma Phys. Control. Fusion*, 2009, *51* 075006 (11pp)